MECSOL 2019 - Proceedings of the 7th International Symposium on Solid Mechanics,
V. Tita, A. Ferreira, M.L. Ribeiro, A. Vieira and A.T. Beck (Editors), ABCM, Sao Carlos, SP, Brazil, April 15th to 17th, 2019

A Sequential Optimization Approach for Honeycomb Crashworthiness using Radial Basis Functions

Matheus Toneli Rodrigues [1], Marco Antônio Luersen [1]

[1] Universidade Tecnológica Federal do Paraná (UTFPR), Rua Deputado Heitor Alencar Furtado, 5000, 81280-340, Curitiba, Paraná, Brasil.

Abstract: Optimization of materials and structures for energy absorption has become an important design topic because of environmental and safety issues. Within this context, this paper proposes a methodology to optimize the out-of-plane crash behavior of honeycombs, well-known structures for their high-energy absorption capacity and low weight. This methodology combines radial basis functions (RBF) with the expected improvement method. Cell size, cell shape and thickness are the design variables. Results show a significant improvement compared to the initial design in terms of the specific energy absorbed, while the peak force values are maintained at low levels. Moreover, the hexagon cell shape seems to have a higher out-of-plane resistance compared to rectangle and auxetic cells.

Keywords: optimization, crash behavior, honeycomb, radial basis functions, expected improvement.

INTRODUCTION

The use of honeycombs as core of sandwich structures or filler of energy absorbers is continuously growing in automotive and aerospace industries. Honeycomb cellular materials have a high strength-to-weight ratio and excellent energy absorbing capacity. Their crushing resistance is influenced by the mechanical properties of wall material, the thickness of the cell wall and the geometric configuration of the cell (Yamashita and Gotoh, 2005; Meran, Toprak and Mugan, 2014). Also, the out-of-plane crushing performance of these structures is higher than the in-plane crushing resistance.

Currently, numerical analysis like finite elements has been used to study the crushing behavior of honeycombs structures. However, a single numerical crushing simulation requires a large computational time. Thus, metamodeling techniques have been applied in the crashworthiness optimization process (Yang et al., 2018; Fazilati and Alisadeghi, 2016; Xie and Zhou, 2015). A surrogate model (or metamodel) is a mathematical approximation that replaces the high fidelity model. Nevertheless, the metamodel built using initial samples obtained from a design of experiments (DOE) will possibly not be accurate in the region of global optimum (Fang et al., 2017). In order to avoid this problem, sequential optimization methods can be applied. These techniques consist of building an initial approximation from a small DOE size and improves the surrogate function in the region of global optimum using some measure until a convergence criterion is met.

Within this context, the present work proposes a methodology to optimize the honeycomb crushing behavior. In this methodology, a surrogate model is improved combining different updating strategies. Radial basis functions (RBF) are used to construct the approximation solution (i.e., the surrogate). RBF were developed for scattered multivariate data interpolation (Hardy, 1971) and have been shown efficient to solve highly nonlinear problems (Fang, Rais-Rohani and Horstemeyer, 2005). In this investigation, the honeycomb structure is modeled using the finite element method (FEM).

CRASHWORTHINESS OPTIMIZATION DESIGN FOR HONEYCOMB STRUCTURES

Finite Element Modeling

The finite element model is built in the commercial code Abaqus to simulate the out-of plane crushing behavior of honeycomb structure as shown in Fig. 1. The explicit method and four-node shell elements (S4R) with six degrees of freedom per node are employed. A rigid plane with a prescribed velocity of 10 m/s is applied for compressing the honeycomb structure (z-direction). A clamped boundary condition with a fully fixed rigid wall is considered in the bottom plane. Self-contact is applied to avoid interpenetration during the folding process of honeycomb walls, while a node-to-surface is prescribed between the honeycomb and the upper plate (Zhang, Zhang and Wen, 2014). A friction coefficient of 0.2 is chosen (Sun et al., 2016). The number of cells of the honeycomb structure is 5x5 and its height (h) is 20 mm.

The honeycomb material is an aluminum alloy AA3003 H18 that is assumed strain-rate independent. This material has Young's modulus E=69 GPa, yield stress σ_y=115.8 MPa, ultimate tensile stress σ_u =154.5 MPa and Poisson's ratio v=0,33. The material hardening is modeled in accordance with Zhang, Zhang and Wen (2014). Concerning the mesh, five elements were used along the cell length and a mesh size of 0.25 mm was adopted in z-direction.

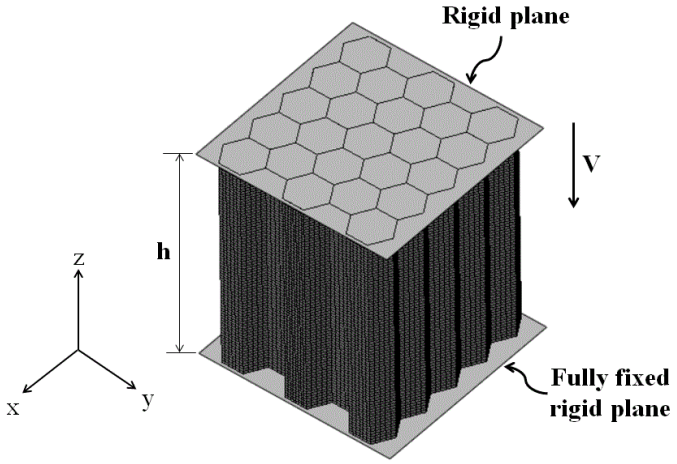

Figure 1 – Numerical model of the honeycomb structure.

Design Criterion and Variables

In this investigation, three design variables are adopted: thickness wall (t), cell length (L) and a cell shape parameter (CS). These variables are defined as illustrated in Fig. 2. The effect of CS on cell configuration is shown in Fig. 3. When CS=1, the cell is a rectangle, the cell assumes an auxetic shape if CS decreases and becomes hexagon if CS values increases. When CS=2, the cell is a regular hexagon. Table 1 presents the initial values of the design variables and their lower and upper bounds.

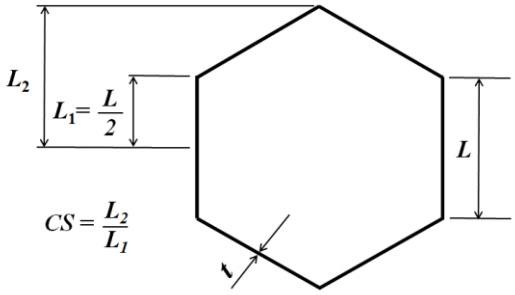

Figure 2 – Design variables.

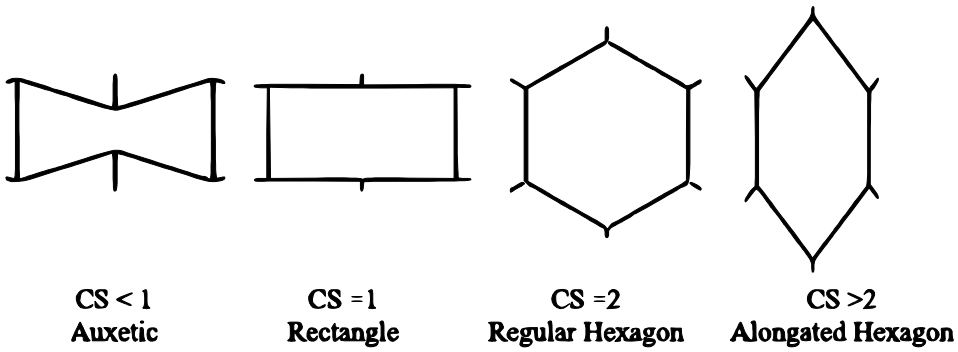

Figure 3 – Influence of cell shape (CS) parameter.

Concerning the objective function, the most agreed design criteria for thin-walled energy absorbers are the specific energy absorbed (SEA) and the peak crush force (PCF) (Baroutaji, Sajjia and Olabi, 2017). The SEA is defined as

$$SEA = \frac{E_a}{m} \tag{1}$$

where E_a and m are the total energy absorbed and the structure mass, respectively. The higher the *SEA*, the better the absorber efficiency. Furthermore, *PCF* is directly related to the deceleration caused by a collision, for example. Thus, the peak crush force needs to be lower than a certain level mainly because of safety reasons. In this work, in the optimization process, *SEA* is the objective function (to be maximized) and a *PCF* value is imposed as a constraint. These parameters can be obtained from the load-displacement diagram. Figure 4 shows a typical honeycomb crush curve, where the area under the curve represents the total energy absorbed by the structure.

In the present investigation, three different optimization cases are performed: one case is unconstrained, i.e. maximization of *SEA* without constraints, while a constraint on the peak force is imposed in the other two cases. The peak crush force for the initial design is adopted to determine the peak force limit (F_{limit}).

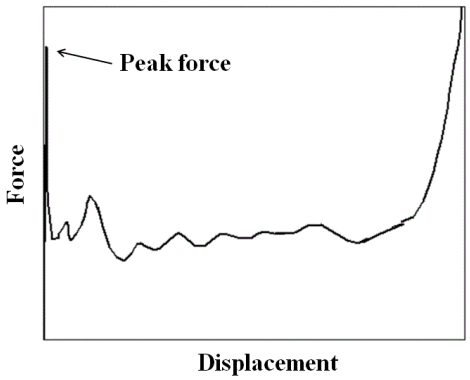

Figure 4 – Typical force vs. displacement crush curve for honeycomb structures.

Table 1 – Bounds and initial values of design variables.

Variable	Bounds		Initial value
	Lower	Upper	
L (mm)	2	5	3.5
t (mm)	0.02	0.1	0.06
CS	0.4	2.73	2

Optimization Procedure

In the optimization procedure proposed, two methods of sequential sampling approaches are applied: the expected improvement (EI) method (Jones et al., 1998) and the minimization of surrogate RBF predictor. The expected improvement method was initially developed with Kriging, but there has been some published work available on EI with RBF (Sóbester, Leary and Keane, 2004; Havinga, Boogaard, Klaseboer, 2017; Li et al., 2010). The RBF technique uses a linear combination of basic functions that are symmetric and centered at each sampling point. For a sample of N designs $\mathbf{X} = \left(\mathbf{x}_1, \mathbf{x}_2 ..., \mathbf{x}_N\right)^T$ and its response vector $\mathbf{y} = \left(y_1, y_2 ..., y_N\right)^T$, the general form of metamodel predictor is given by

$$\hat{y} = \hat{f}(\mathbf{x}) = \sum_{i=1}^{N} \lambda_i \phi\left(\left\|\mathbf{x} - \mathbf{x}_i\right\|\right) \tag{2}$$

where $\left\|\mathbf{x} - \mathbf{x}_i\right\|$ is the Euclidian distance between $\mathbf{x}$ and the sampling point $\mathbf{x}_i$, ϕ is a basis function and λ_i is the unknown weighting factor positioned at $\mathbf{x}_i$. The unknown coefficient vector $\boldsymbol{\lambda} = \left(\lambda_1, \lambda_2 ..., \lambda_N\right)^T$ is determined by

$$\mathbf{y} = \boldsymbol{\Phi}\boldsymbol{\lambda} \tag{3}$$

In this equation, $\Phi_{ij} = \phi\left(\left\|\mathbf{x}_i - \mathbf{x}_j\right\|\right)$, where $i, j = 1, 2 ..., N$. Different types of basis function can be considered. In order to facilitate the derivation of an expected improvement measure, the exponentially decaying Gaussian basis function is adopted over this work:

$$\phi(r) = e^{-r^2/2\sigma^2} \tag{4}$$

where $r = \|\mathbf{x} - \mathbf{x}_i\|$ and σ is a parameter that controls the region of influence of each kernel and, consequently, can influence the surrogate model accuracy.

Because the metamodel is an approximation of the true function, it may be difficult to find the optimum value using only the initial sampling data in a surrogate-based optimization. It is recommended to enhance the surrogate accuracy in promising regions of design space by adding new points (infill points) to the initial sampling data. According to Forrester, Sóbester and Keane (2008), applying infill points at the optimum predicted by the metamodel is a way to rapidly converge to an optimum value. However, this may not lead to the global optimum, because the searching process can get trapped at a local minimum region, for example. In order to avoid this problem, the minimization of surrogate RBF predictor is combined with the maximum expected improvement method. The expected improvement at a point **x** for a Gaussian process is written as

$$EI(\mathbf{x}) = \begin{cases} \left(y_{mín} - \hat{y}(\mathbf{x})\right)\Psi\left(\dfrac{y_{mín} - \hat{y}(\mathbf{x})}{\hat{s}(\mathbf{x})}\right) + \hat{s}(\mathbf{x})\psi\left(\dfrac{y_{mín} - \hat{y}(\mathbf{x})}{\hat{s}(\mathbf{x})}\right), & \text{if } \hat{s}(\mathbf{x}) > 0 \\ 0\ , & \text{if } \hat{s}(\mathbf{x}) = 0 \end{cases} \tag{5}$$

where Ψ and ψ are, respectively, the standard normal distribution function and the standard normal density function. Also, $\hat{s}(\mathbf{x})$ is the metamodel error estimate and $y_{mín} = \min\left[y_1, y_2 ..., y_N\right]$. The expected improvement will be large at a point where the predicted value is smaller than $y_{mín}$ and where there is much uncertainty associated with the prediction. To compute the estimated error of the RBF predictor, it is assumed that $y(\mathbf{x})$ is in fact the realization of some Gaussian stochastic process $Y(\mathbf{x})$. Using a Gaussian distribution of N responses $y(\mathbf{x})$, Sóbester, Leary and Keane (2004) show that the mean and the variance of the assume process at $\mathbf{x}_{N+1}$ are, respectively:

$$\hat{y}_{N+1}(\mathbf{x}) = \boldsymbol{\phi}\boldsymbol{\Phi}^{-1}\mathbf{y}^T \tag{6}$$

$$\sigma^2{}_{N+1}(\mathbf{x}) = 1 - \boldsymbol{\phi}\boldsymbol{\Phi}^{-1}\boldsymbol{\phi}^T \tag{7}$$

where $\boldsymbol{\phi} = \left[\phi\left(\|\mathbf{x}_{N+1} - \mathbf{x}_1\|\right), \phi\left(\|\mathbf{x}_{N+1} - \mathbf{x}_2\|\right) ... \phi\left(\|\mathbf{x}_{N+1} - \mathbf{x}_N\|\right)\right]$ and $\sigma(\mathbf{x}) = \hat{s}(\mathbf{x})$. Equation (5) does not take in account constraints. For constrained optimization problems, $EI(\mathbf{x})$ needs to be multiplied by the probability of the constraint being met:

$$P\left[g(\mathbf{x}) < c\right] = \Psi\left(\frac{c - \hat{g}(\mathbf{x})}{s_g(\mathbf{x})}\right) \tag{8}$$

where $\hat{g}(\mathbf{x})$, c and s_g are, respectively, the constraint predictor, the constraint limit and the estimated metamodel prediction error for the constraint function. Note that the constraint is written in the form $g(\mathbf{x}) < c$ in Eq. (8). For the present work, the constraint is represented by

$$PCF - F_{\text{limit}} \leq 0 \tag{9}$$

Thus, $g(\mathbf{x}) = PCF - F_{\text{limit}}$, c=0 and the expected improvement is given by $EI(\mathbf{x}) \cdot P\left[g(\mathbf{x}) < 0\right]$. The optimization procedure proposed uses alternatively the expected improvement and minimization of RBF predictor. For constrained and unconstrained problems, the algorithm steps can be summarized as follows:

1. Generate initial N samples with a Latin hypercube DOE and get their corresponding objective function values.
2. Determine the optimal parameter σ of RBF with leave-one-out cross validation procedure. After data normalization, the problem domain of searching for parameter is over the range $[10^{-1},10^{1}]$, and 20 values of σ logarithmically spread over the range are considered and the Rippa's formula is applied to reduce the computational complexity of this method (Fasshauer and Zhang, 2007).
3. Obtain an infill point. At this step, a new infill point is obtained alternatively by two different ways. One method is to use the optimal point of the current optimization interaction to update the model. A genetic algorithm is applied to minimize the approximate function. Another method is to maximize the EI, using a simulated annealing algorithm. At each interaction, only one method is applied and only one infill point is added.

4. Update the surrogate model with the infill point obtained in step 3 and its corresponding objective function value. σ is calculated again.
5. The optimization procedure should be terminated when the number of interactions exceeds a predefined limit.

NUMERICAL RESULTS AND DISCUSSION

In this section, the results of the numerical cases formulated in subsection "Design Criterion and Variables" are presented and discussed, i.e. the maximization of the specific energy absorbed with or without a peak crush force constraint. For each problem, a total of 50 points (finite elements evaluations) were used: 10 points generated initially by the Latin hypercube method and 40 infill points. The results for the initial design and the optimal designs are summarized in Tab. 2. Note that the force limit (F_{limit}) represents 50% (Case 2) and 30% (Case 3) of the peak force value exhibited by the initial design.

Table 2 – Optimization results.

Case	Constraint	Optimal design variables			*SEA* (kJ/kg)	*PCF* (kN)	Initial design	
		L	*t*	CS			*SEA* (kJ/kg)	*PCF* (kN)
1	-	2	0.1	2.14	15.5	2.71	8.97	2.95
2	0.5 x $PCF_{initial}$	2	0.054	1.91	11.3	1.47		
3	0.3 x $PCF_{initial}$	2	0.032	1.76	8.8	0.88		

From Tab. 2, it can be observed that, when there is no constraint, the optimum design has the highest thickness value and the lowest cell length value, what is in accordance with some authors (e.g., Meran, Toprak and Mugan, 2014; Xie and Zhou, 2015). Also, the best designs still have the lowest cell length value for constrained cases. Compared to the initial design, *SEA* increased 73.0%, and 25.5% in cases 1 and 2, respectively. Although there is no constraint in case 1, the peak force is lower than the initial *PCF* value. Regarding the cell shape, notice that all optimal designs have a hexagon cell with a small variation compared to the initial design (regular hexagon). Figure 5 shows the evolution of the objective function for Case 1. Note that algorithm needed only two iterations to find the optimum design. Figure 6 represents the evolution of the objective function in each iteration and the best feasible objective function of the initial sampling set for Case 2. The corresponding constraint values (*PFC*) are shown in Fig. 7.

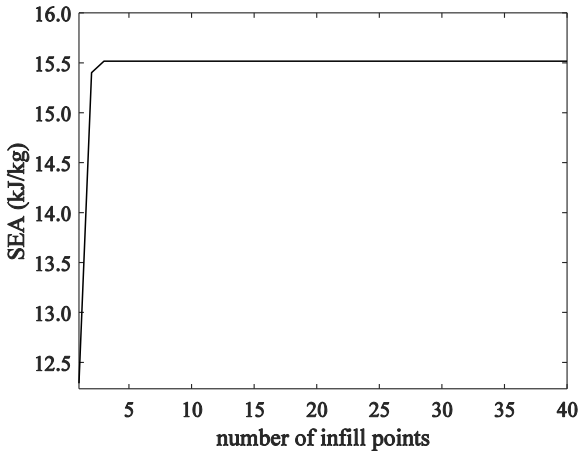

Figure 5 – Evolution of the objective function (Case 1).

Figure 6 shows a significant increase of *SEA* (over 50%) relative to the initial best design, represented by the blue dot. It can be noticed in Fig. 7 that 16 points of 40 are located in the infeasible region, although the optimum solution, found after only few iterations, satisfies the constraint. Two reasons can explain why infeasible designs are obtained by the optimization process. First, the metamodel of the objective function and/or the surrogate of the constraint are not sufficiently accurate and, consequently, a feasible point for the predictor may not be a feasible point for the real function. Second, a starting point may be generated in the infeasible region and the search algorithm (simulated annealing or genetic) stays in it. Moreover, poor solutions are generated even after applying a good number of infill points, what suggests the problem is multimodal with presence of multiple local minimum.

Figure 8 illustrates the evolution of the objective function for Case 3 in each iteration and the best feasible objective function of the initial sampling set. The corresponding constraint values (*PFC*) are shown in Fig. 9. All points generated by the DOE are located in the infeasible region in Case 3. Nevertheless, the optimum design was found after adding few

infill points. Note that the number of points out of feasible region increased compared to Case 2. This occurs because the constraint is stricter in Case 3. The difficulty of finding feasible solutions demonstrates the benefit of applying infill strategies.

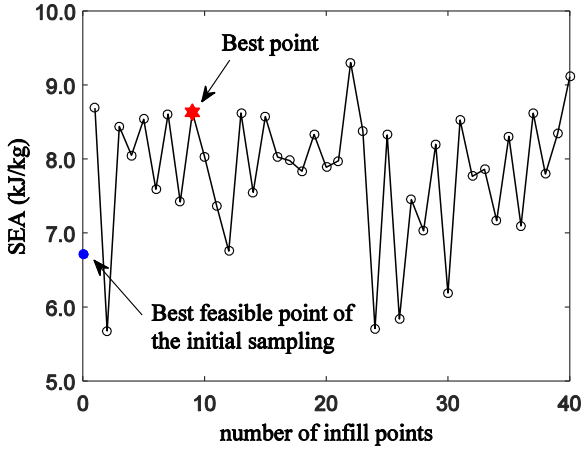

Figure 6 – Evolution of the objective function (Case 2).

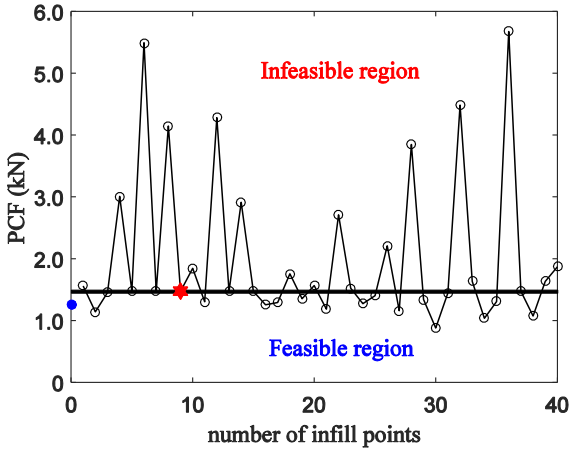

Figure 7 – Evolution of the constraint (Case 2).

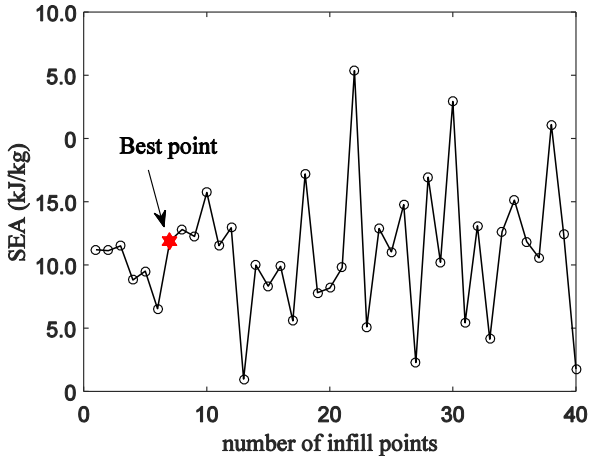

Figure 8 – Evolution of the objective function (Case 3).

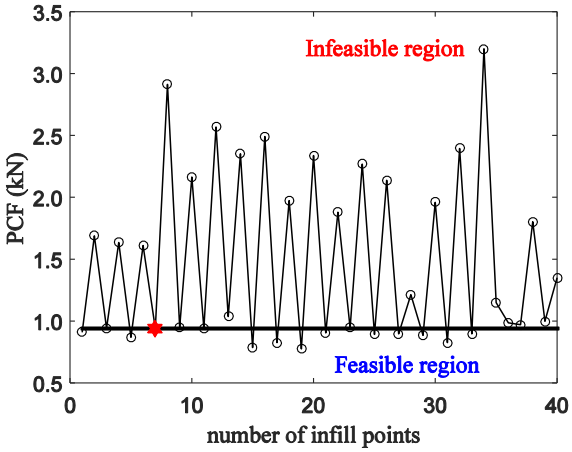

Figure 9 – Evolution of the constraint (Case 3).

CONCLUSIONS

In this work, the main goal was to apply and test a methodology to optimize the crashworthiness of honeycomb structures, using RBF with the expected improvement method and the minimization of the predictor. Concerning the numerical results, the optimum solutions improved the initial design in terms of *SEA* and the constraints were satisfied. In addition, the hexagon cell seems to have a higher out-of-plane performance compared to rectangle and auxetic cells. From the perspective of the proposed surrogate-based optimization strategy, the algorithm was shown to have a satisfactory performance, once good solutions were obtained quickly from an affordable computational budget. It is important to mention that the proposed methodology can be applied to other optimization problems with continuous variables. Lastly, the next step of the present research is to use the methodology to perform a multiobjective optimization study with honeycomb structures.

ACKNOWLEDGMENTS

The authors gratefully acknowledge the support from CAPES.

REFERENCES

Fang, H., Rais-Rohani, M., Liu, Z. and Horstemeyer, M.F., 2005, “A comparative study of metamodeling methods for multiobjective crashworthiness optimization”, Computers & Structures, Vol. 83, pp. 2121-2136.

Fang, J., Sun, G., Qiu, N., Kim, N.H. and Li, Q., 2017, “On design optimization for structural crashworthiness and its state of the art”, Structural and Multidisciplinary Optimization, Vol. 55, pp. 1091-1119.

Fasshauer, G.E. and Zhang, J.G., 2007, “On choosing ‘optimal’ shape parameters for RBF approximation”, Numerical Algorithms, Vol. 45, pp. 345-368.

Fazilati, J. and Alisadeghi, M., 2016. Multiobjective crashworthiness optimization of multi-layer honeycomb energy absorber panels under axial impact. Thin-Walled Structures, Vol. 107, pp. 197-206.

Hardy, R.L., 1971, “Multiquadric equations of topography and other irregular surfaces”, Journal of geophysical research, Vol. 76, pp. 1905-1915.

Havinga, J., van den Boogaard, A.H. and Klaseboer, G., 2017, “Sequential improvement for robust optimization using an uncertainty measure for radial basis functions”, Structural and multidisciplinary optimization, Vol. 55, pp. 1345-1363.

Jones, D.R., Schonlau, M. and Welch, W.J., 1998, “Efficient global optimization of expensive black-box functions”. Journal of Global optimization, Vol. 13, pp. 455-492.

Li, C., Wang, F.L., Chang, Y.Q. and Liu, Y., 2010, “A modified global optimization method based on surrogate model and its application in packing profile optimization of injection molding process”, The International Journal of Advanced Manufacturing Technology, Vol. 48, pp. 505-511.

Meran, A.P., Toprak, T. and Muğan, A., 2014, “Numerical and experimental study of crashworthiness parameters of honeycomb structures”, Thin-Walled Structures, Vol. 78, pp. 87-94.

Sóbester, A., Leary, S.J. and Keane, A.J., 2004, “A parallel updating scheme for approximating and optimizing high fidelity computer simulations”, Structural and multidisciplinary optimization, Vol. 27, pp. 371-383.

Sun, G., Jiang, H., Fang, J., Li, G. and Li, Q., 2016, “Crashworthiness of vertex based hierarchical honeycombs in out-of-plane impact”, Materials & Design, Vol. 110, pp. 705-719.

Xie, S. and Zhou, H., 2015. Analysis and optimisation of parameters influencing the out-of-plane energy absorption of an aluminium honeycomb. Thin-Walled Structures, Vol. 89, pp. 169-177.

Yamashita, M. and Gotoh, M., 2005, "Impact behavior of honeycomb structures with various cell specifications—numerical simulation and experiment", International Journal of Impact Engineering, Vol. 32, pp. 618-630.

Yang, C., Xu, P., Yao, S., Xie, S., Li, Q., and Peng, Y, 2018. Optimization of honeycomb strength assignment for a composite energy-absorbing structure. Thin-Walled Structures, Vol. 127, pp. 741-755.

Zhang, X., Zhang, H. and Wen, Z., 2014, "Experimental and numerical studies on the crush resistance of aluminum honeycombs with various cell configurations", International Journal of Impact Engineering, Vol. 66, pp. 48-59.

RESPONSIBILITY NOTICE

The authors are the only responsible for the printed material included in this paper.